AN UPDATE ON BIAXIAL THERMAL CREEP OF VANADIUM ALLOYS – R. J. Kurtz (Pacific Northwest National Laboratory)*, A. M. Ermi, (COGEMA Engineering Corp.), and H. Matsui (Tohoku University).

OBJECTIVE

To determine the biaxial thermal creep characteristics of V-4Cr-4Ti and V-3Fe-4Ti over the temperature range 650 to 800°C at realistic stress levels. The results will be compared with uniaxial creep tests in vacuum being carried out at Argonne National Laboratory [1] and biaxial creep experiments in lithium being performed at Oak Ridge National Laboratory [2] to determine the effect of interstitial oxygen on creep properties.

SUMMARY

A study of the thermal creep properties of two vanadium alloys was performed using pressurized tube specimens. Creep tubes nominally 4.57 mm OD by 0.25 mm wall thickness were pressurized with high-purity helium gas to mid-wall effective stresses below the effective (Von Mises) yield strength. Specimens were fabricated from V-4Cr-4Ti (Heat No. 832665) and a V-3Fe-4Ti alloy. The samples were heated to 650, 700, 725, and 800°C in an ultra-high vacuum furnace and periodically removed to measure the change in tube outer diameter with a high-precision laser profilometer. The normalized minimum creep rate $(\dot{\varepsilon}kT/DGb)$ was found to be power-law dependent on the modulus compensated applied stress (σ/G). The value of the stress exponent varied with the applied stress. At normalized stresses ranging from 2 to 8×10^{-3} the stress exponent was about 4 and the activation energy was about 300 kJ/mole, which is quite close to the activation energy for self-diffusion in pure vanadium. These results suggest that the predominant mechanism of creep in this regime is climb-assisted dislocation motion. At lower stresses the value of the stress exponent is near unity suggesting that viscous creep mechanisms such as Coble creep or grain boundary sliding may be operative, but the data are too sparse to be conclusive. The reported creep rates from uniaxial tests [1] in vacuum are several times higher than the creep rates measured here. This is probably due to the larger interstitial oxygen concentration of the creep tubing (699 wppm) compared to the sheet stock (310 wppm) used for tensile specimen fabrication. Finally, the creep strength of V-4Cr-4Ti at 700 and 800°C was superior to the V-3Fe-4Ti alloy.

PROGRESS AND STATUS

The procedure for specimen preparation and testing has been described in detail previously [3]. Since the most recent report [4] considerable additional data has been obtained on the creep characteristics of V-4Cr-4Ti, and an additional vanadium alloy, V-3Fe-4Ti. The matrix of materials, test temperatures and stress levels that has been explored is shown in Table 1. All testing has been completed at 700 and 800°C. Only specimens at 650 and 725°C are currently under test.

Results and Discussion

The effective strain-time data for the 650 and 725°C specimens are listed in Table 2. Tables 3 and 4 give the same type of data for pressurized tubes tested at 700 and 800°C, respectively. The time dependence of the effective mid-wall strain is plotted in Figures 1 – 4 for V-4Cr-4Ti

* Pacific Northwest National Laboratory (PNNL) is operated for the U.S. Department of Energy by Battelle Memorial Institute under contract DE-AC06-76RLO-1830.

Table 1. Unpressurized creep tube dimensions, fill pressures and mid-wall effective stress levels.

Test Temperature, °C	Alloy	Specimen Code	Specimen OD, mm	Specimen Wall, mm	Fill Pressure, MPa	Mid-Wall Effective Stress, MPa
650	V-4Cr-4Ti	AR01	4.5665	0.2504	7.922	175.0
		AR02	4.5686	0.2560	9.308	200.1
		AR03	4.5668	0.2530	11.556	250.0
		AR04	4.5690	0.2550	13.093	279.9
		AR06	4.5669	0.2520	13.886	300.1
		AR07	4.5651	0.2560	15.884	335.1
700	V-4Cr-4Ti	AR11	4.5674	0.2601	2.896	66.5
		AR12	4.5662	0.2532	3.909	91.4
		AR13	4.5672	0.2456	4.937	118.5
		AR14	4.5657	0.2499	5.930	138.9
		AR15	4.5659	0.2553	6.964	158.8
	V-3Fe-4Ti	NB01	4.5712	0.2146	3.268	91.8
		NB02	4.5700	0.1753	3.730	129.2
		NB03	4.5789	0.2073	5.592	160.6
725	V-4Cr-4Ti	AR08	4.5646	0.2477	6.205	150.0
		AR09	4.5667	0.2586	7.846	180.0
		AR10	4.5677	0.2428	8.156	200.0
800	V-4Cr-4Ti	AR16	4.5684	0.2477	2.654	70.6
		AR17	4.5667	0.2507	3.571	92.6
		AR18	4.5664	0.2461	4.482	117.7
		AR19	4.5667	0.2543	5.419	136.8
		AR20	4.5659	0.2527	1.793	47.6
		AR21	4.5679	0.2454	0.910	26.4
	V-3Fe-4Ti	NB05	4.5692	0.1882	2.055	74.0
		NB06	4.5669	0.2139	2.979	92.2

Table 2. Time dependence of effective mid-wall creep strain for 650 and 725°C tests.

	Specimen Code								
	650°C						725°C		
Time, h	AR01	AR02	AR03	AR04	AR06	AR07	AR08	AR09	AR10
144	-	-	-	1.8425	-	-	-	-	-
190	0.0151	0.0223	1.2427	-	2.2417	3.7172	0.0694	0.4905	0.6075
313	-	-	-	1.8729	-	-	-	-	-
330	-	-	-	-	-	-	-	-	3.4775
334	0.0172	0.0275	1.2531	-	2.2883	4.0141	0.1560	2.8212	
385	-	-	-	-	-	-	-	3.8558	
483	-	-	-	1.9031	-	-	-		
503	0.0187	0.0169	1.2592	-	2.3590	4.6455	0.3027		
651	-	-	-	1.9916	-		-		
673	0.0193	0.0406	1.2879	-	2.8959		0.5310		
820	-	-	-	2.0396	-		-		
841	0.0262	0.0567	1.3069	-	3.2688		1.6045		
988	-	-	-	2.1186	-		-		
1010	0.0367	0.0697	1.3182	-	3.7093		3.0028		
1178	0.0317	0.0732	1.3447	-	4.8321		4.3460		

Table 3. Time dependence of effective mid-wall creep strain for 700°C tests.

	Specimen Code							
Time, h	AR11	AR12	AR13	AR14	AR15	NB01	NB02	NB03
101	-	-	-	-	-	0.0650	0.0578	0.3314
168	0.0072	0.0000	0.0072	0.0072	0.0217	-	-	-
242	0.0072	0.0000	0.0072	0.0145	0.0361	-	-	-
357	0.0072	0.0072	0.0072	0.0289	0.0795	-	-	-
478	-	-	-	-	-	0.4546	0.3826	5.6911
585	-	-	-	-	-	0.6278	0.5486	12.165
598	0.0072	0.0217	0.0145	0.0578	0.2096	-	-	
752	-	-	-	-	-	0.9884	0.9382	
919	-	-	-	-	-	1.3921	1.3204	
1110	-	-	-	-	-	1.8605	1.8178	
1277	-	-	-	-	-	2.3791	2.2357	
1375	0.0072	0.0145	0.0217	0.1229	0.9246	-	-	
1523	0.0072	0.0000	0.0361	0.1373	1.2783	-	-	
1661	-	-	-	-	-	3.6456	3.6395	
1997	-	-	-	-	-	5.7723	5.3574	
2157	0.0361	0.0289	0.0578	0.3468	4.5424	-	-	
2362	-	-	-	-	-	7.5867	6.9435	
2780	0.0289	0.0217	0.0578	0.8596	10.247	-	-	
2804	-	-	-	-	12.956	-	-	
2842	-	-	-	-		10.585	9.3220	
2881	0.0289	0.0361	0.0867	0.9896		-	-	
3258	0.0289	0.0217	0.0867	1.5309		-	-	
3273	-	-	-	-		13.533	11.760	
3365	0.0361	0.0289	0.0939	1.6896				
3418	-	-	-	-		-	-	
3532	0.0289	0.0289	0.0939	2.1008		17.040	12.688	
3653	-	-	-	-			14.414	
3699	0.0289	0.0361	0.1011	2.3676			-	
3827	-	-	-	-			15.885	
3887	-	-	-	-			17.269	
3890	0.0217	0.0361	0.1445	2.7712				
4057	0.0217	0.0361	0.1300	3.1820				
4441	0.0289	0.0506	0.1806	4.1036				
4777	0.0361	0.0578	0.2312	5.4847				
5142	0.0506	0.0650	0.2817	6.6126				
5622	0.0361	0.0650	0.3756	8.3490				
6053	0.0506	0.0650	0.4623	9.9534				
6198	0.0795	0.0723	0.5200	10.763				
6433	0.0433	0.1228	0.5922	12.564				
6607	0.0361	0.0723	0.6716	14.199				
6667	0.0650	0.0867	0.6933	14.798				
7267	0.0578	0.1012	0.9604					
8029	0.0578	0.1156	1.3428					
8772	0.0722	0.1301	1.7756					
9663	0.0650	0.1445	2.3019					

Table 4. Time dependence of effective mid-wall creep strain for 800°C tests.

Time, h	Specimen Code							
	AR21	AR20	AR16	AR17	AR18	AR19	NB05	NB06
101	-	-	-	-	-	-	-	20.024
144	-	-	-	-	-	-	1.3495	
167	0.0072	0.0000	-	-	-	-	-	
168	-	-	0.0289	0.0650	0.1445	3.5917	-	
242	-	-	0.0361	0.1156	0.6212	14.709	-	
358	0.0217	0.0217	-	-	-		-	
412	-	-	0.1156	0.8089	5.7999		-	
427	-	-	-	-	-		6.8442	
488	-	-	0.1806	1.5306	10.832			
516	0.0217	0.0434	-	-	-			
578	-	-	0.3466	2.9363	24.141			
727	-	-	0.8375	6.4173				
864	-	-	1.5156	13.561				
900	0.0578	0.2312	-					
1031	-	-	2.6327					
1236	0.0795	0.5202	-					
1343	-	-	5.4454					
1491	-	-	7.1108					
1601	0.1300	1.0329	-					
1784	-	-	10.835					
2081	0.2095	1.8483	-					
2125	-	-	16.000					
2333	0.2311	2.3458	-					
2460	-	-	21.295					
2668	0.3033	3.1025	-					
2812	-	-	26.827					
2903	0.3539	3.6787	-					
2956	-	-	29.201					
3077	0.3683	4.0818	-					
3137	0.3972	4.2545	-					
3239	-	-	33.912					
3346	-	-	35.806					
3513	-	-	38.907					
3680	-	-	42.279					
3737	0.5199	5.9371	-					
3871	-	-	46.557					
4029	-	-	51.885					
4499	0.6860	8.0689						
5242	0.8736	10.304						
6052	1.0613	12.735						

specimens tested at 650, 700, 725 and 800°C, respectively. Figure 5 gives a plot of the strain-time data for V-3Fe-4Ti at 700°C. It is interesting that the 650°C creep curves all display "classical" features in that a distinct primary creep regime is found, followed by a steady-state creep region, and finally an accelerating creep rate to failure. In contrast, the creep curves at 700, 725 and 800°C show an accelerating creep rate almost from the beginning of the test. No primary creep was observed and the duration of the steady-state regime was very brief. Similar results have been found for biaxial creep tests in lithium [5] but not for the uniaxial tests in vacuum [4]. The occurrence of a continuously accelerating creep rate almost from the onset of testing is not due to specimen geometry effects. Wheeler [6] found an accelerating creep curve for ultrahigh vacuum tests of pure vanadium at temperatures below 925°C but not at higher

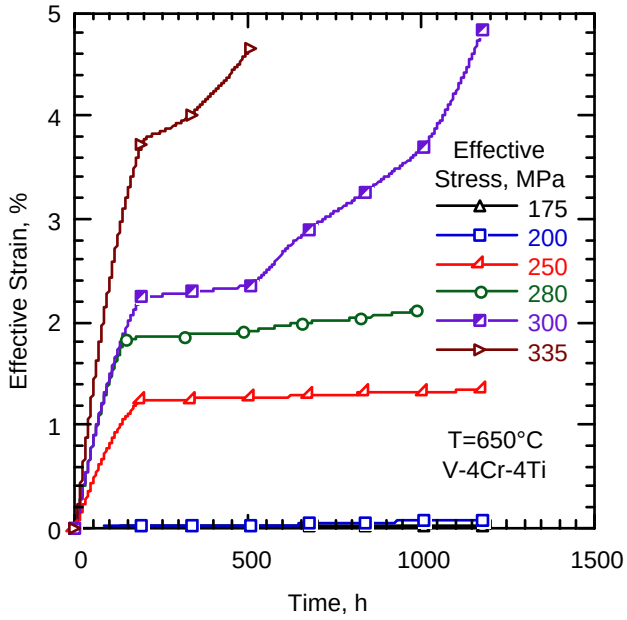

Figure 1. Time dependence of the normalized effective mid-wall creep strain at 650°C for unirradiated V-4Cr-4Ti.

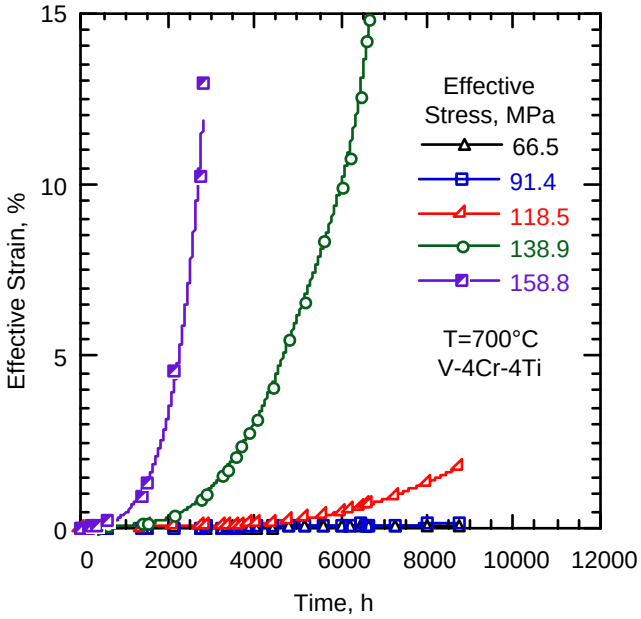

Figure 2. Time dependence of the normalized effective mid-wall creep strain at 700°C for unirradiated V-4Cr-4Ti.

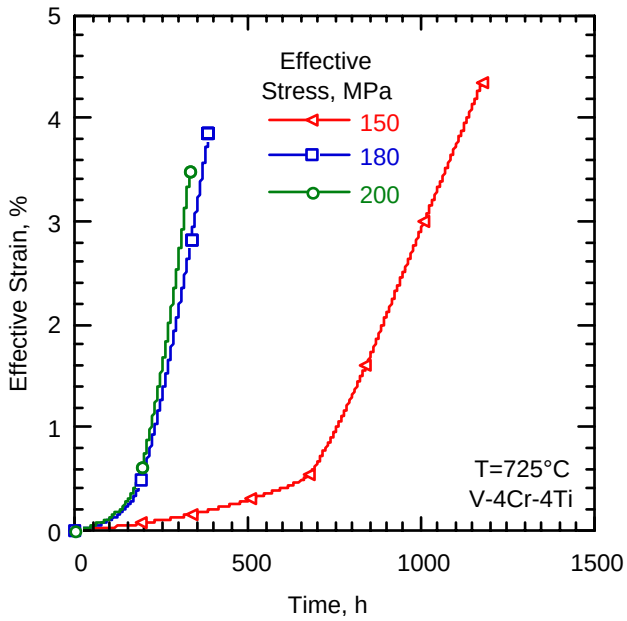

Figure 3. Time dependence of the normalized effective mid-wall creep strain at 725°C for unirradiated V-4Cr-4Ti.

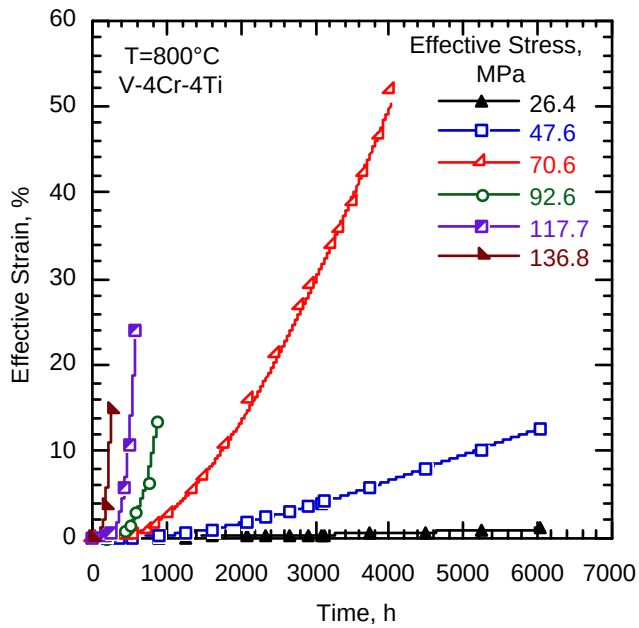

Figure 4. Time dependence of the normalized effective mid-wall creep strain at 800°C for unirradiated V-4Cr-4Ti.

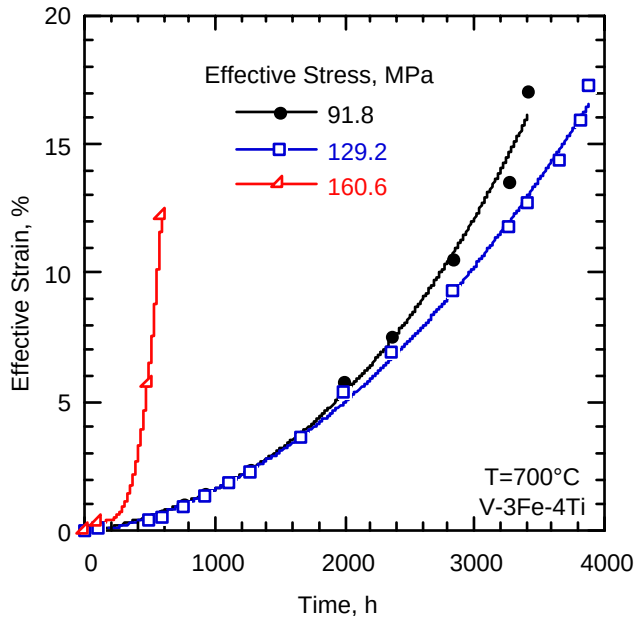

Figure 5. Time dependence of the normalized effective mid-wall creep strain at 700°C for unirradiated V-3Fe-4Ti.

temperatures. Accelerating creep curves are not uncommon and can be observed in most metals and alloys [7].

Effective minimum creep rates were obtained from the strain-time data taking care to exclude the portions of the curves that showed primary or tertiary creep behavior. Typically the effective minimum creep rates were determined at effective strain levels less than about 0.2%. Normalized effective creep rates were then calculated from:

$$\dot{\varepsilon}_N = \frac{\dot{\varepsilon} kT}{DGb} \qquad (1)$$

where $\dot{\varepsilon}$ is the effective minimum creep rate, k is Boltzmann's constant, T is the absolute temperature, D is the self-diffusion coefficient, G is the elastic shear modulus and b is the Burgers vector. The normalized effective creep rates were plotted against the normalized stress, which was obtained by dividing the applied stress by the shear modulus. Values of the shear modulus as a function of temperature were determined from [8]:

$$G = \left(0.488 - 8.43x10^{-5}\,T\right)x10^{11} \qquad (2)$$

where T is the absolute temperature. Equation 2 is valid only for pure vanadium but recent research [9] on the elastic properties of V-5Cr-5Ti indicates that the shear modulus of this particular alloy differs from pure vanadium by less than 1% at 300K. The temperature dependence of the self-diffusion coefficient was computed from [7]:

$$D = D_o \exp\left[\frac{-Q}{RT}\right] \qquad (3)$$

where the pre-exponential term, D_o, was assumed to be $1x10^{-6}$ and the activation energy, Q, was taken as 270 kJ/mole.

A log-log plot of the normalized effective minimum strain rate against the normalized stress is given in Figure 6 for the biaxial and uniaxial [1] creep experiments performed in vacuum. The data clearly shows that the stress dependence of the creep rate (and therefore the predominant creep mechanism) varies with stress. At low stresses ($<2x10^{-3}$) the stress exponent is near unity which is indicative of a viscous creep mechanism such as Coble creep or grain boundary sliding. The data are too few to reach a firm estimate at what stress these mechanisms become operative. At intermediate stresses (2 to $8x10^{-3}$) the stress exponent is around 4 which suggests that a climb-assisted dislocation glide mechanism dominates the creep process. Finally, at high stresses ($>8x10^{-3}$) the stress exponent is very large (>10) which is representative of the power-law breakdown regime.

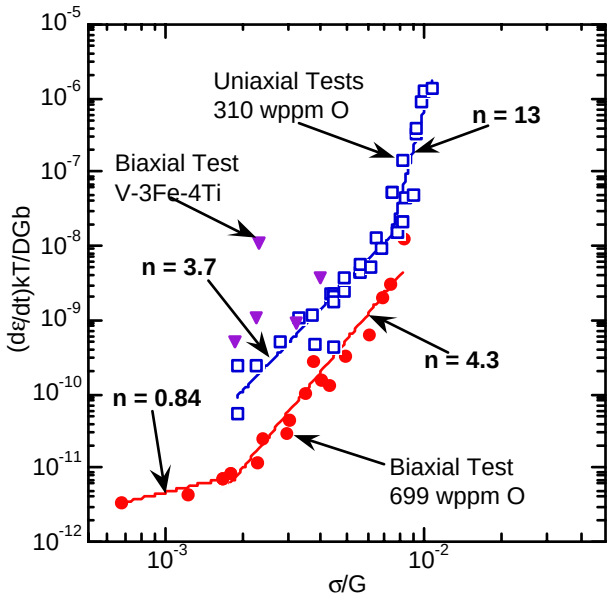

Figure 6. Stress dependence of the normalized effective mid-wall creep strain for unirradiated vanadium alloys.

It is evident from Figure 6 that the creep rate of the uniaxial specimens is substantially greater than the biaxial specimens. Part of this difference may be due to texture effects associated with the tube microstructure compared to sheet tensile specimens. While such an effect could account for some of the difference it is not known if the creep tubing exhibits any significant texture. A more likely source of the difference is the different interstitial oxygen concentration of the creep tubes versus the tensile specimens. The sheet stock used to make the uniaxial creep specimens had a starting interstitial oxygen concentration of 310 wppm, whereas the initial creep tube oxygen level is much higher at 699 wppm. Since the steady-state creep regime is very short duration in these tests it is expected that oxygen pickup during the test is not a concern. Such differences in interstitial oxygen can produce dramatic changes in the creep rate of pure vanadium. Schirra [10] has shown that increasing the oxygen concentration from 220 to 750 wppm decreased the creep rate by five orders of magnitude. The effect of interstitial oxygen on creep of V-Ti alloys was smaller than pure vanadium, but on the same order as the findings reported here [10].

Also shown in Figure 6 are creep data for V-3Fe-4Ti pressurized creep tubes. With the exception of one data point the stress dependence of the creep rate is similar to V-4Cr-4Ti, but there is far too few data to reliably compute a meaningful stress exponent. The data clearly show that the creep rate of this alloy is significantly greater than that of V-4Cr-4Ti.

A comparison of the creep-rupture performance of various vanadium alloys is presented in Figure 7 which shows a Larsen-Miller parameter plot of the available data. The Larsen-Miller parameter was computed from:

$$P = \frac{T(\log t_r + 20)}{1000} \qquad (4)$$

where T is the absolute temperature and t_r is the time-to-rupture in hours. V-Cr-Ti alloys containing 10 to 15% Cr are included in Figure 7 to illustrate the superior creep-rupture resistance of vanadium alloys with chromium levels greater than 4 to 5% [11]. There is generally good correlation between the uniaxial test results of Chung et al., [12] and Natesan et al. [1] and the biaxial creep results generated in this study. Evidently differences in interstitial oxygen concentration did not significantly influence the time-to-rupture. The good correlation may be fortuitous since oxygen pickup during the course of a long term test is expected to affect creep ductility and, therefore, time-to-rupture. In addition, the uniaxial tests employed constant loading so the gauge section stress increases during the experiment as the specimen cross-section decreases. In contrast, as a pressurized tube expands the gas pressure decreases yielding a roughly constant effective stress for mid-wall strains up to about 20%. Note the creep-rupture performance of V-3Fe-4Ti is generally inferior to the V-Cr-Ti alloys.

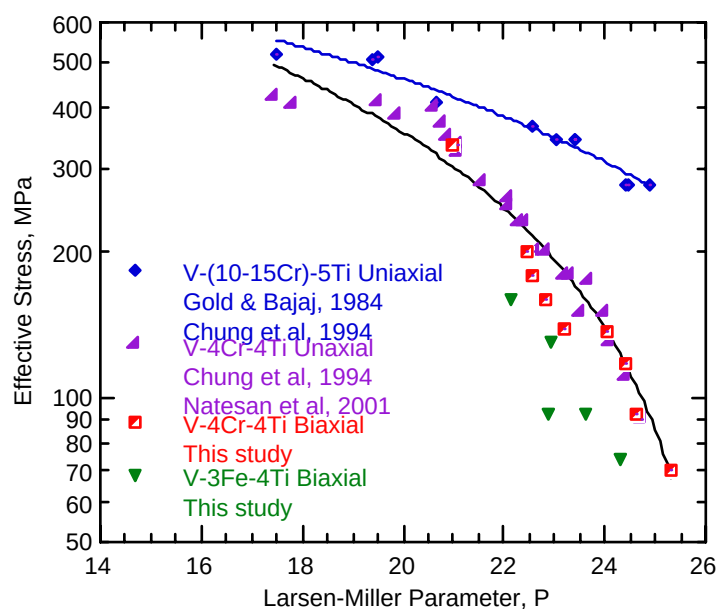

Figure 7. Larsen-Miller parameter plot for creep rupture of unirradiated vanadium alloys.

Conclusions

An on-going study of the thermal creep properties of V-4Cr-4Ti is being performed using pressurized tube specimens. The normalized minimum creep rate was found to be power-law dependent on the modulus compensated applied stress. The value of the stress exponent varied

with the applied stress. At normalized stresses ranging from 2 to $8x10^{-3}$ the stress exponent was about 4 and the activation energy was about 300 kJ/mole, which is quite close to the activation energy for self-diffusion in pure vanadium. These results suggest that the predominant mechanism of creep in this regime is climb-assisted dislocation motion. At lower stresses the value of the stress exponent is near unity suggesting that viscous creep mechanisms such as Coble creep or grain boundary sliding may be operative. The reported creep rates from uniaxial tests are several times higher than the creep rates measured here. This is probably due to differences in interstitial oxygen concentration at the beginning of the test. Finally, the creep strength of V-4Cr-4Ti at 700 and 800°C was superior to the V-3Fe-4Ti alloy.

ACKNOWLEDGEMENTS

We acknowledge the significant efforts of L. K. Fetrow and R. M. Ermi in performing the experiments described in this report.

REFERENCES

[1] K. Natesan, W. K. Soppet and D. L. Rink, "Uniaxial Creep Behavior of V-4Cr-4Ti Alloy," in Fusion Materials: Semiannual Progress Report for Period Ending December 31, 2000, DOE/ER-0313/29 (2001) 37.

[2] M. L. Grossbeck, "Biaxial Thermal Creep of V-4Cr-4Ti in a Lithium Environment," in Fusion Materials: Semiannual Progress Report for Period Ending June 30, 2001, DOE/ER-0313/30 (2001) 8.

[3] R. J. Kurtz and M. L. Hamilton, “Biaxial Thermal Creep of V-4Cr-4Ti at 700°C and 800°C,” in Fusion Materials: Semiannual Progress Report for Period Ending December 31, 1998, DOE/ER-0313/25 (1999) 7.

[4] R. J. Kurtz and M. L. Hamilton, "Biaxial Thermal Creep of V-4Cr-4Ti at 700°C and 800°C," *J. of Nuc. Matls*. 283-287 (2000) 628.

[5] M. L. Grossbeck, "Biaxial Creep of V-4Cr-4Ti in a Lithium Environment," submitted for publication in the proceedings of the 10th International Conference on Fusion Reactor Materials.

[6] R. K. Wheeler, E. R. Gilbert, F. L. Yaggee and S. A. Duran, *Acta Metal*. Vol. 19 (1971) 21.

[7] D. L. Harrod and R. E. Gold, *Int. Metals Rev.* 4 (1980) 163.

[8] R. J. Farraro and R. B. McLellan, “High Temperature Elastic Properties of Polycrystalline Niobium, Tantalum and Vanadium,” *Met. Trans.* 10A (1979) 1699.

[9] W. D. Porter, R. B. Dinwiddie, W. A. Simpson, and M. L. Grossbeck, “Determination of the Thermophysical Properties of V-5Cr-5Ti,” ANL/FPP/TM-287 (1994) 41.

[10] M. Schirra, “Das Zeitstandfestigkeits und Kriechverhalten von Vanad-Basis Legierungen,” KFK Report 2440, Kernforschungszentrum Karlsruhe (1989).

[11] R. E. Gold and R. Bajaj, *J. of Nucl. Mater*. 122-123 (1984) 759.

[12] H. M. Chung, B. A. Loomis and D. L. Smith, *J. of Nucl. Mater*. 212-215 (1994) 772.